

RESEARCH MEMORANDUM

USE OF SHOCK-TRAP BLEED TO IMPROVE PRESSURE RECOVERY
OF FIXED - AND VARIABLE - CAPTURE - AREA INTERNAL -
CONTRACTION INLETS; MACH NUMBER 2.0 TO 3.0

By Roger W. Luidens and Richard J. Flaherty

Lewis Flight Propulsion Laboratory
Cleveland, Ohio

Declassified April 23, 1962

**NATIONAL ADVISORY COMMITTEE
FOR AERONAUTICS**

WASHINGTON

August 14, 1958

NATIONAL ADVISORY COMMITTEE FOR AERONAUTICS

RESEARCH MEMORANDUM

USE OF SHOCK-TRAP BLEED TO IMPROVE PRESSURE RECOVERY
OF FIXED- AND VARIABLE-CAPTURE-AREA INTERNAL-
CONTRACTION INLETS; MACH NUMBER 2.0 TO 3.0 *

By Roger W. Luidens and Richard J. Flaherty

SUMMARY

Two internal-contraction inlets were investigated in the NACA Lewis laboratory 1- by 1-foot block tunnel. The fixed inlet was tested at Mach 2.94 with a conventional ram-scoop bleed and with a "shock-trap" bleed. The shock-trap bleed is a scoop bleed with an area expansion starting upstream of the leading edge of the scoop. This bleed system improved the inlet pressure recovery 0.09 at a constant 28-percent bleed flow.

At a free-stream Mach number of 2.94, the variable-capture-area inlet gave a peak pressure recovery of 0.91 at a diffuser Mach number of 0.47 and 29-percent bleed. The pressure recovery in the bleed was 0.62; thus the bleed drag was estimated, as being 3.5 percent of engine thrust, under favorable assumptions. This inlet gave pressure recoveries of 0.89 at Mach numbers of 1.98 and 2.43.

INTRODUCTION

The all-external-compression inlet is theoretically limited in its pressure-recovery potential, as is discussed in reference 1. This limiting pressure recovery decreases as the flight Mach number increases. Also, inlets designed for this potential recovery have large cowl-pressure drags. The internal-contraction inlet on the other hand has a pressure-recovery potential of 100 percent with zero cowl-pressure drag. Reference 2 reports an investigation of an all-internal-contraction inlet which had the contraction divided between a centerbody and the outer walls of the duct. The inlets of the present report have all internal contraction but no centerbody.

A fixed- and a variable-capture-area inlet each with a design Mach number of 3.0 are reported herein. The compression surface for the fixed-capture-area inlet was a right circular truncated cone. This inlet was tested with a ram scoop and a "shock-trap" bleed. The shock-trap bleed is a scoop bleed with an area expansion starting upstream of the leading

edge of the scoop. The function of this bleed is to reduce the relatively high pressure losses resulting from terminal-shock - boundary-layer interaction in an all-internal-compression inlet.

The variable-capture-area inlet had approximately the same geometry as the fixed-capture-area inlet at Mach 3.0. The airflow characteristics of this inlet over the range of flight Mach numbers from 0 to 3.0 would be expected to match closely those of a turbojet engine operating at nearly constant corrected rotational speed (or constant compressor-inlet Mach number). A study of an inlet that is similar but has a supersonic diffuser of rectangular cross section is reported in reference 3.

APPARATUS AND PROCEDURE

The investigation was conducted in the NACA Lewis laboratory 1- by 1-foot block tunnel at the following conditions:

Mach number	Total pressure, lb	Total temperature, °F
	sq in. abs	
1.98	16	100
2.45	25	↓
2.94	25	↓

The specific humidity was maintained sufficiently low to avoid condensation effects.

A general sketch of the fixed-capture-area inlet and instrumentation is shown in figure 1. Further details of the throat bleed systems are given in figure 2. The shock-trap bleed is distinguished from the ram-scoop bleeds by the area expansion that starts ahead of the leading edge of the scoop. A shim could be inserted at the throat section of the supersonic diffuser, as shown in figure 2. This increased the contraction of the inlet and decreased the height of the bleed gap.

In conducting the tests the inlet was started by opening and then closing the "starting door" which controlled the airflow through a longitudinal slot in the supersonic diffuser. After the inlet was started the mass-flow plug was closed until maximum pressure recovery was obtained. The mass flow passing through the subsonic diffuser was computed from the total head rakes and the assumption of a choked exit area. The capture mass

flow was determined from the free-stream conditions and the inlet capture area. The engine mass-flow ratio is the ratio of the mass passing through the subsonic diffuser to the capture mass flow. The bleed mass-flow ratio is 1 minus the engine mass-flow ratio.

A sketch of the variable-capture-area inlet and instrumentation is shown in figure 3. One jaw of the inlet could be fixed at a given angle to the subsonic diffuser. The angle of the other jaw could be remotely controlled. At each test Mach number trial runs were made to determine the angle of the fixed jaw which resulted in the axis of the supersonic and subsonic diffuser being coincident and aligned with the free stream at the maximum contraction ratio. This procedure was found necessary to achieve the highest pressure recovery. A shim similar to that of the first model could also be used with this model. The throat bleed was always operated as a shock-trap bleed. In conducting this test the inlet capture area was reduced until the inlet started (supersonic flow was established in the supersonic diffuser), and then was increased until the inlet unstopped. The inlet was then restarted and the capture area increased to just less than that which unstopped the inlet. The exit plug was then closed to determine maximum pressure recovery.

Pressure recovery was measured on two rakes. The front and back rakes were 2 and 17 throat diameters downstream of the throat, respectively (see figs. 1 and 3). The bleed-duct rake was 0.75 of a throat diameter downstream of the throat (see fig. 3).

RESULTS AND DISCUSSION

Fixed-Capture-Area Inlet

The longitudinal distribution of the local static pressure as a fraction of free-stream total pressure for the supersonic and subsonic diffuser is shown in figure 4 for the fixed-capture-area inlet at peak pressure recovery with two types of bleed. The estimated sonic static-pressure ratio is also shown on the figure. The data indicate that the terminal shock for the ram-scoop bleed was a shock train located in the subsonic diffuser. The marked increase in static pressure at the entrance to the subsonic diffuser for the shock-trap bleed, on the other hand, shows that the terminal shock train was collected into a single shock and trapped in the bleed gap with this type bleed. Adding the shim shown in figure 2 covered some static orifices in the 8- to 10-inch axial distance region and prevented the collection of these pressures for two of the inlet configurations.

The inlet total-pressure recoveries for the fixed-capture-area inlet are shown in figure 5. These recoveries were measured on the back rakes where the profiles were in all cases flat. For all three bleed geometries the capture mass flow was the same; thus a decrease in engine mass flow results from a corresponding increase in bleed flow.

The inlets with ram-scoop bleeds would operate only supercritically, that is, only at constant engine flow corresponding to movement of the terminal shock within the subsonic diffuser. The decreasing mass flow at the higher pressure recoveries for the shock-trap bleed resulted from increased spillage through the bleed associated with movement of the terminal shock upstream of the entrance to the subsonic diffuser but within the bleed gap. At the identical mass-flow ratios of 0.72 (hence also identical bleed flows of 28 percent), the pressure recovery for the shock-trap bleed was 0.85 compared with 0.76 for the ram-scoop bleed, a 0.09 improvement. This improvement in pressure recovery and the slight regulation of the mass flow at high recovery appear characteristic of the shock-trap bleed.

Several schlieren photographs of the throat bleed gap are presented in figure 6. The parts of the figure correspond to the letters labeling the data points in figure 5. The terminal shock moves from the downstream end to the upstream end of the bleed gap with decreasing engine mass flow.

The following explanation is offered for the favorable effect of the shock-trap bleed type on inlet pressure recovery. For the inlet with the shock-trap bleed the step in the bleed formed a rapidly diverging area in which the terminal shock train could collect and stand without unstating the inlet. Expansion waves sufficiently weakened the terminal shock so that the boundary layer entered the bleed duct against little or no adverse pressure gradient and without the terminal-shock loss in total pressure. When the inlet with the ram-scoop bleed is at peak pressure recovery, there is a shock train in the diverging subsonic diffuser with a concomitant total-pressure loss. Closing the exit plug farther causes the first leg of the shock train to move into the converging supersonic diffuser where it is unstable and causes the inlet to unstart.

Variable-Capture-Area Inlet

The pressure recoveries of the inlet at Mach 2.94 for two variations in the bleed system are shown in figure 7. The peak pressure recovery was 0.91 with a diffuser Mach number of 0.47. The back-rake pressure recovery for this model was 0.88 compared to 0.85 for the fixed-area model at a mass-flow ratio of 0.71 (29-percent bleed flow). There was a marked decrease in pressure recovery as the bleed flow was reduced.

The front-rake total-pressure profiles for the points labeled on figure 7 are shown in figure 8 with corresponding letters. The data points at the walls on figure 8 are wall static pressures. The mass-flow ratio, average total-pressure ratio, and approximate local Mach number are shown on the figure.

Profile A is for supersonic flow through the entire subsonic diffuser. The data show that the boundary layer is very thin. This indicates

complete or nearly complete removal of the boundary layer developed in the supersonic diffuser. The dip in the profile at the center could be due to the coalescence of oblique shocks in the supersonic diffuser into a normal shock. This condition can be shown to exist by the method of characteristics (ref. 4).

Profile B is the maximum-distortion profile. The tubes next to the wall have large pressure defects. This indicates that the boundary layer has thickened because of the adverse pressure gradient caused by throttling the subsonic diffuser exit. It is hypothesized that this profile is strongly influenced by the terminal-shock train. The shock train is made up of a series of "lambda" shocks, each of which has a pair of oblique shocks near the walls and a normal shock near the center of the duct. The high-pressure-recovery annulus is associated in part with the higher efficiency of the oblique shocks.

Profile C shows that further throttling increased the recovery and also the boundary-layer thickness. If all the boundary layer in the supersonic diffuser has been removed, this could only be due to the boundary layer that has developed in the subsonic diffuser interacting with the terminal-shock train. The terminal-shock train in this case occurs farther upstream in the subsonic diffuser, at a lower supersonic Mach number, and is probably of shorter length.

With further throttling the shock train coalesces in the shock-trap bleed. Under this circumstance shock - boundary-layer interaction is avoided and the boundary layer is thinner (profiles D and E). Based on the experimentally determined maximum-contraction ratio and an estimation of the boundary-layer displacement thickness and pressure recovery, the Mach number at the end of the supersonic diffuser is about 1.45. The total-pressure recovery across a normal shock at Mach 1.45 is 0.95. For a measured average maximum recovery of 0.91, this leaves 0.04 for oblique-shock losses and subsonic friction losses.

Bleed-duct profiles of static to free-stream total pressure, pitot-pressure ratio, and the corresponding calculated values of total-pressure recovery are presented in figure 9. The flow in the bleed duct was supersonic. The bleed pressure recoveries should be regarded with caution because they depend on static-pressure measurements that were difficult to make accurately. The high pressure recoveries are located toward the inner side of the duct, as would be expected from the consideration of the main-duct boundary-layer profile that enters the bleed. The peak total-pressure recovery in the bleed duct at supercritical main-duct flow is 0.92, a value consistent with the high recoveries observed in the main duct. The average bleed recovery is 0.62.

From the bleed-duct mass flow and total-pressure recovery a bleed drag coefficient may be calculated. The bleed flow was assumed to be

expanded to ambient pressure and discharged in the free-stream direction. For the inlet and the data of profile E (fig. 8) the drag coefficient based on the cross-sectional area of the free-stream tube of air that enters the subsonic diffuser (or engine) had a value of 0.035. The thrust coefficient of a turbojet engine at an afterburner temperature of 3000° R, based on the same area as the drag coefficient just mentioned, is about 1.0. The bleed drag was thus about 3.5 percent of the engine thrust. Hence, the drag of the large bleeds need not be excessive under the most favorable conditions. (A discharge angle, or over- or underexpansion, would increase the drag.) This type of inlet could be designed for zero-cowl-pressure drag at the design Mach number.

The performance of the variable-capture-area inlet at other Mach numbers is given in figure 10 for peak pressure recovery. Also presented are the average bleed-duct pressure recovery, the inlet mass-flow ratio, and a calculated bleed drag coefficient, which is previously defined. It was found that to get maximum pressure recovery it was necessary to keep the axes of the supersonic and subsonic diffusers coincident and aligned with the free stream. The bleed-duct geometry ratios were $s/r = h/r = l/r = 0.2$ (see fig. 2). The inlet gave peak pressure recoveries of 0.89 at Mach numbers of 1.98 and 2.43, compared with the value of 0.91 at Mach 2.94.

A schematic drawing of the inlet geometries at all Mach numbers is shown in figure 11. It is evident that for the lower Mach numbers the inlet has more internal wetted area than an optimum inlet design. Also shown in figure 11 are the experimental maximum geometric inlet contraction ratio and the isentropic contraction at each Mach number. The geometric contraction ratio is defined as the ratio of the capture area of the supersonic diffuser to its discharge area. The geometric value is about 82 percent of the isentropic value at each Mach number. The aerodynamic contraction ratio is greater than the geometric contraction ratio by the boundary-layer displacement area.

SUMMARY OF RESULTS

The experiments on internal-contraction inlets with several types of bleed may be summarized as follows:

1. The use of a bleed, termed a shock-trap bleed, which eliminates terminal-shock - boundary-layer interaction improved the recovery of an internal-contraction inlet from 0.76 with a throat ram-scoop bleed to 0.85 at Mach 2.94. The shock-trap bleed also permitted some regulation of the engine mass flow at high pressure recovery.

2. A peak pressure recovery of 0.91 with a diffuser Mach number of 0.47 was obtained at a free-stream Mach number of 2.94 on a variable-capture-area inlet with a shock-trap bleed duct diverting 29 percent of the air entering the supersonic inlet. This inlet gave pressure recoveries of 0.89 at Mach 1.98 and 2.43.

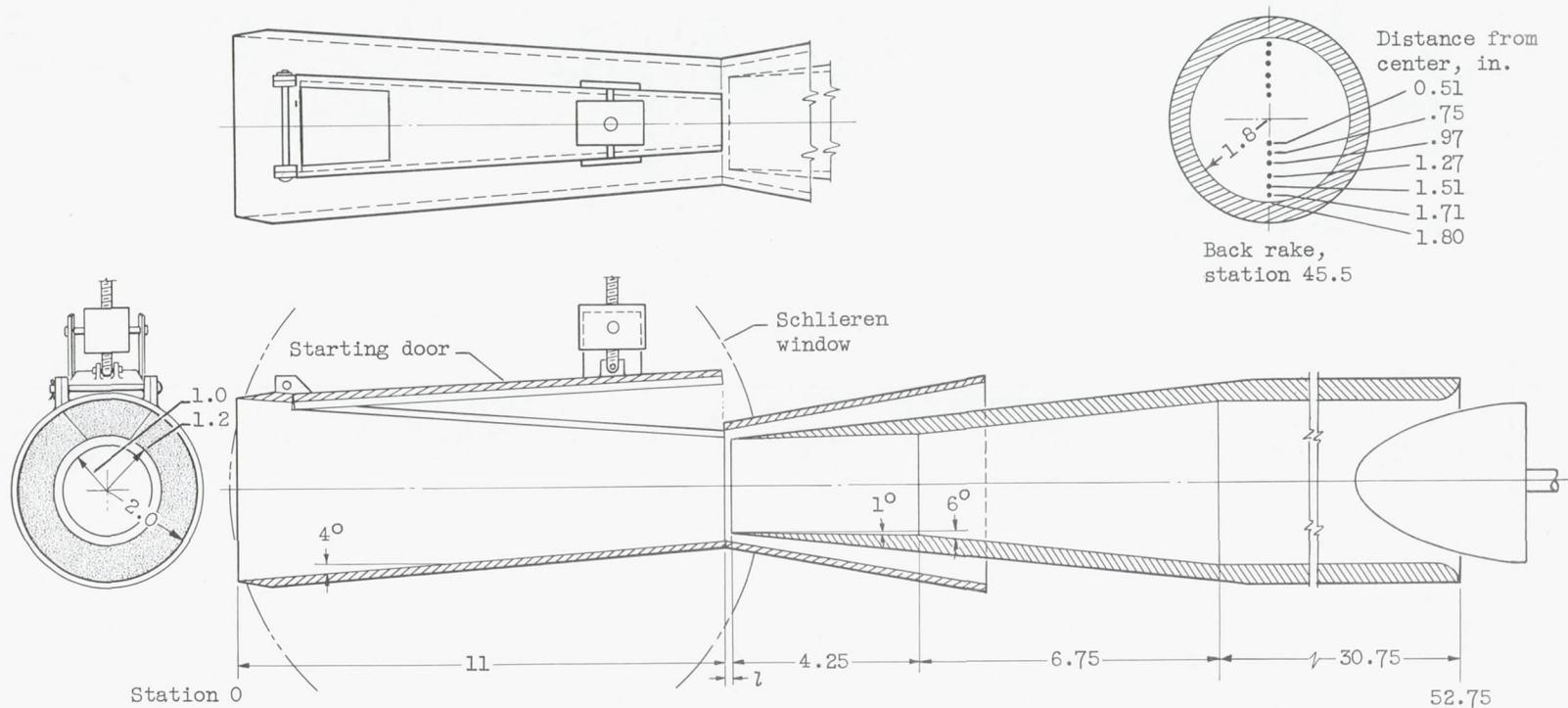
3. Although the bleed flow with the shock-trap bleed was large, the total-pressure recovery in the bleed duct was high (0.62); this resulted in an estimated drag of 3.5 percent of the engine thrust at Mach 2.94.

4. To achieve maximum pressure recoveries it was found necessary to keep the axes of the subsonic and supersonic diffusers coincident and aligned with the free stream.

Lewis Flight Propulsion Laboratory
National Advisory Committee for Aeronautics
Cleveland, Ohio, May 8, 1958

REFERENCES

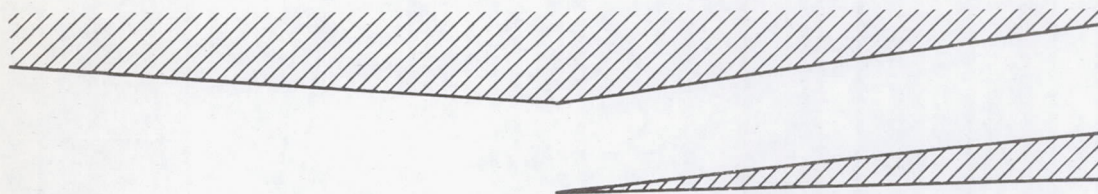
1. Connors, James F., and Meyer, Rudolph C.: Design Criteria for Axisymmetric and Two-Dimensional Supersonic Inlets and Exits. NACA TN 3589, 1956.
2. Mossman, Emmet A., and Pfyl, Frank A.: An Experimental Investigation at Mach Numbers from 2.1 to 3.0 of Circular-Internal-Contraction Inlets with Translating Centerbodies. NACA RM A56G06, 1956.
3. Gunther, Fred C., and Carr, John H.: Development of an Adjustable Supersonic Inlet Utilizing Complete Boundary-Layer Removal at the Throat. Prog. Rep. No. 20-321, Jet Prop. Lab. C.I.T., June 14, 1957. (Contract DA-04-ORD-18.)
4. Ferri, Antonio: Application of the Method of Characteristics to Supersonic Rotational Flow. NACA Rep. 841, 1946. (Supersedes NACA TN 1135.)



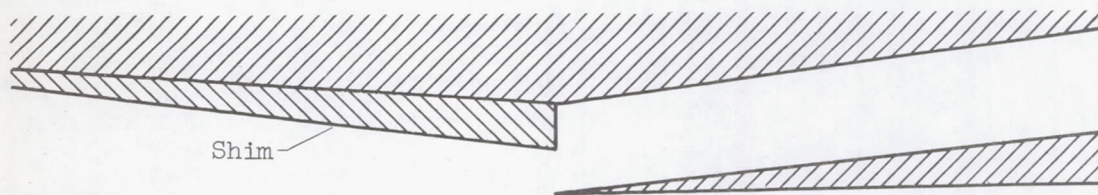
Ten static taps spaced 1.0 inch part starting at station 1.5 (in supersonic diffuser)
 Five static taps spaced 1.0 inch apart starting 0.75 inch downstream of leading edge of
 subsonic diffuser

CD-6089

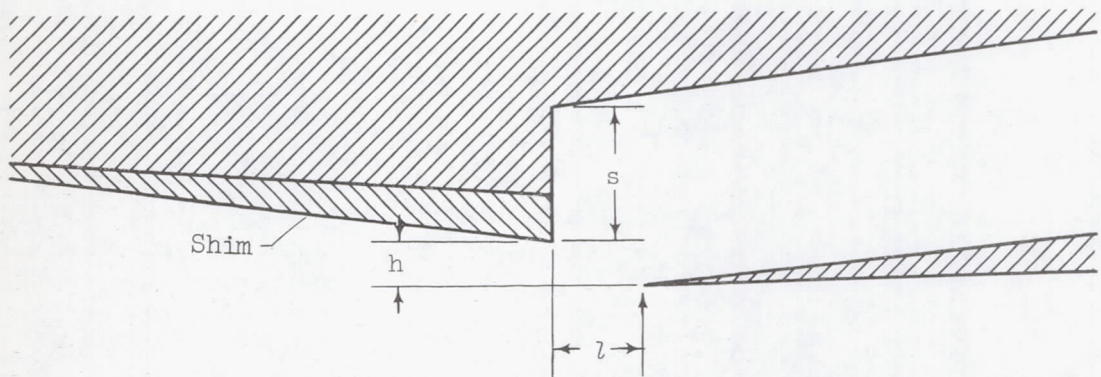
Figure 1. - Drawing of fixed-capture-area-inlet model and instrumentation. (All dimensions in inches.)



(a) Ram-scoop bleed; $l/r, 0$; $h/r, 0.2$; $s/r, 0$.



(b) Ram-scoop bleed; $l/r, 0$; $h/r, 0.1$; $s/r, 0.1$.



r (Radius of subsonic-diffuser inlet)

(c) Shock-trap bleed; $l/r, 0.2$; $h/r, 0.1$; $s/r, 0.3$.

Figure 2. - Details of the bleed system for fixed-capture-area-inlet model and definition of terms for bleed geometry.

4857

CW-2

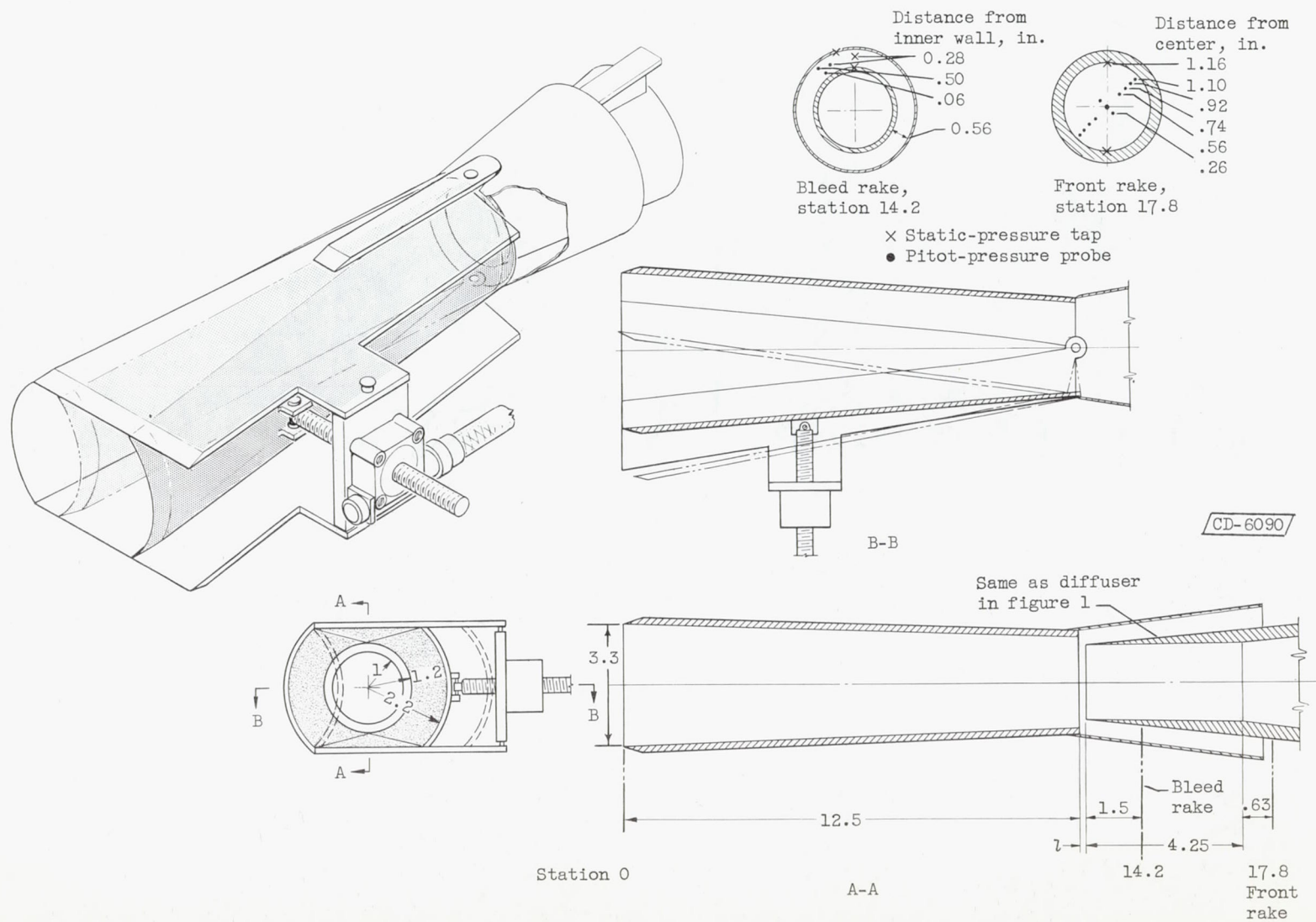


Figure 3. - Drawing of variable-capture-area-inlet model and instrumentation. (All dimensions in inches.)

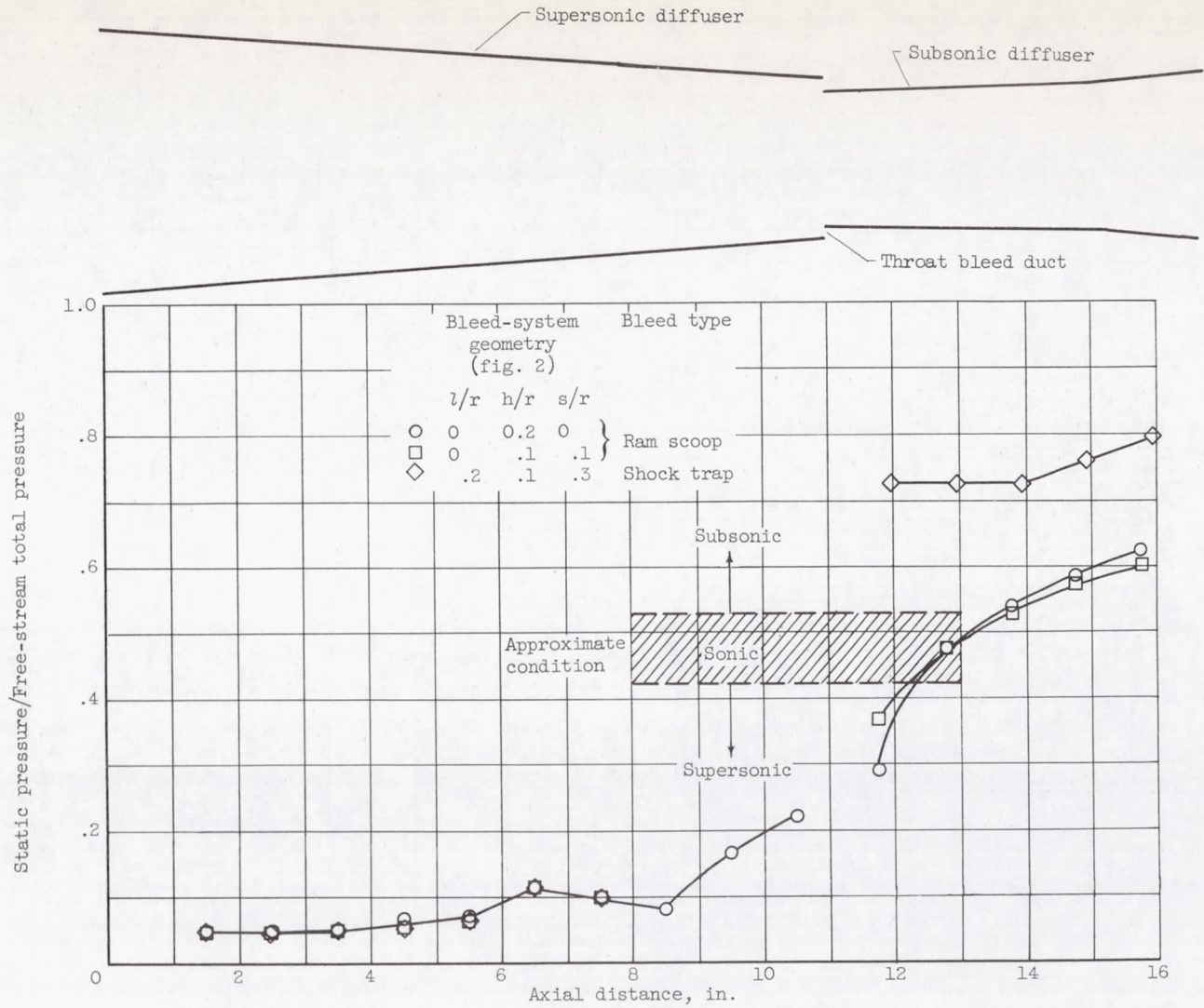


Figure 4. - Longitudinal static-pressure distribution in fixed-capture-area inlet. Mach number, 2.94; data are for peak-pressure-recovery points.

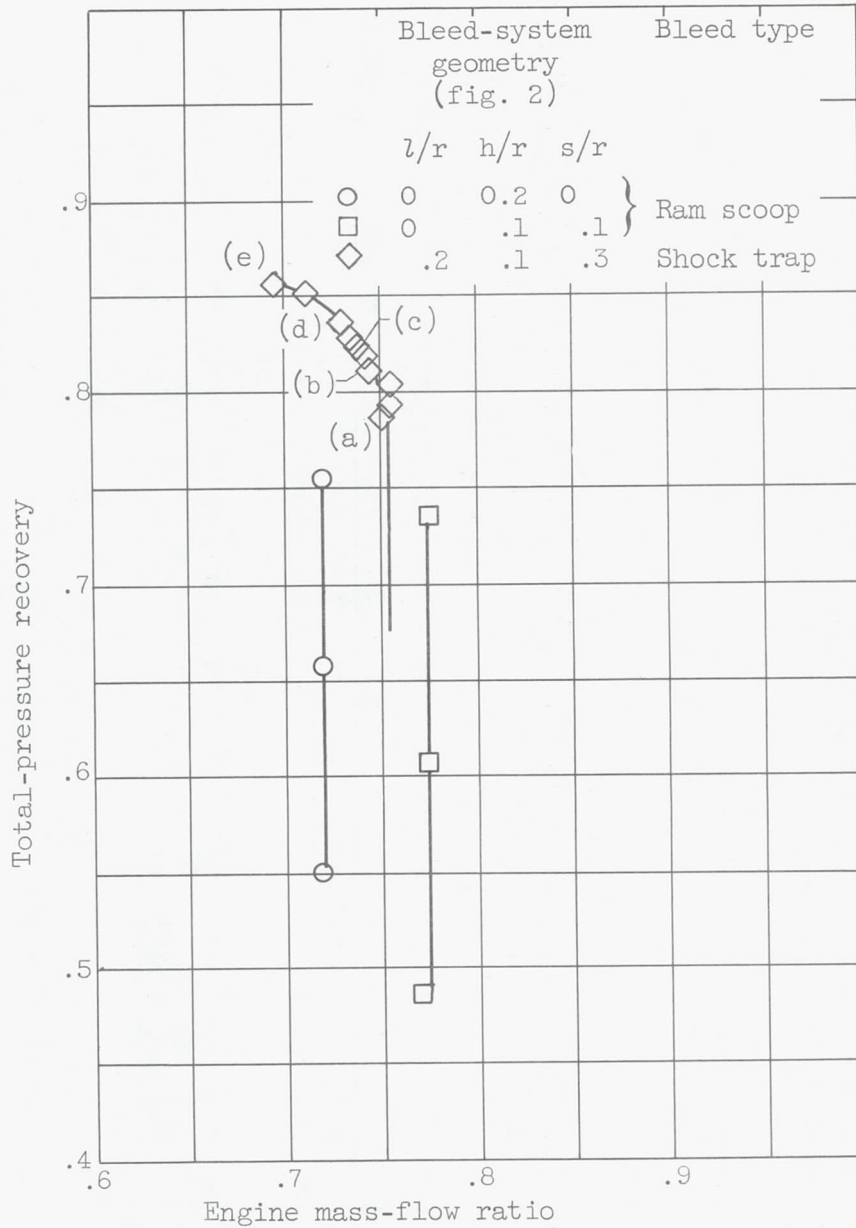
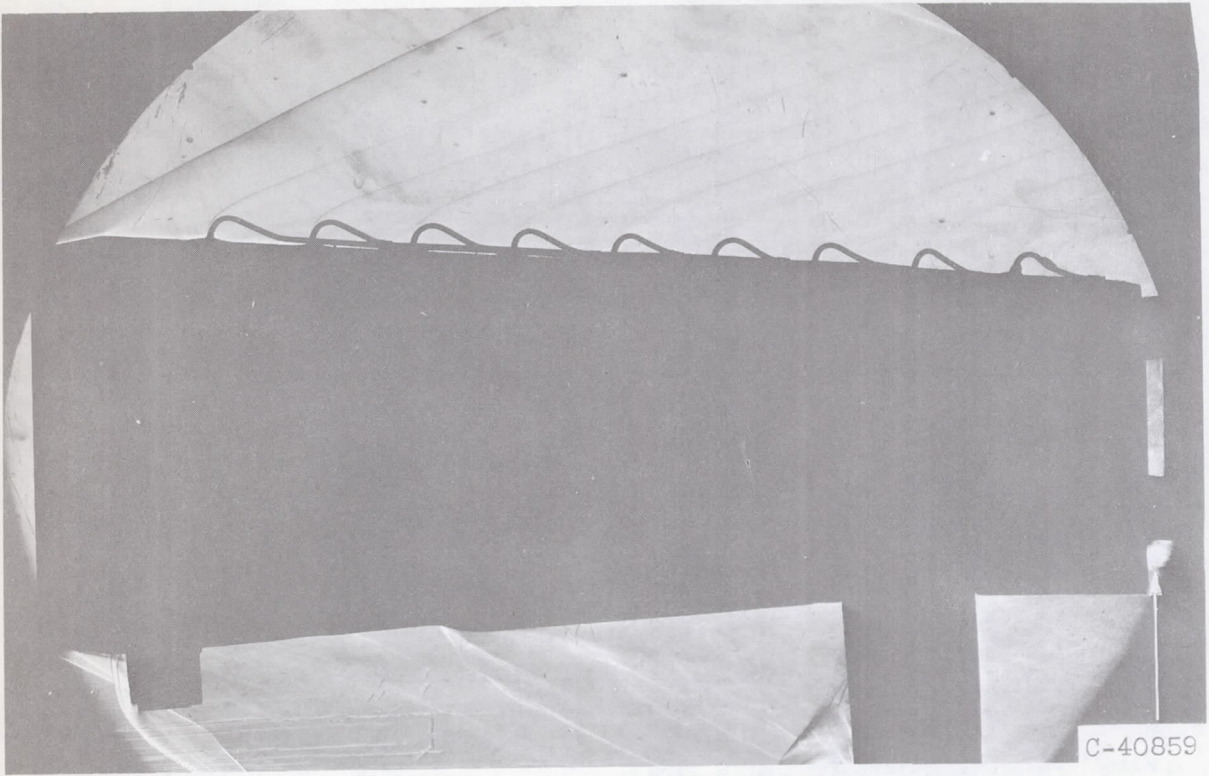


Figure 5. - Back-rake total-pressure recovery for fixed-capture-area inlet. Mach number, 2.94. (Letters refer to parts of figure 6.)

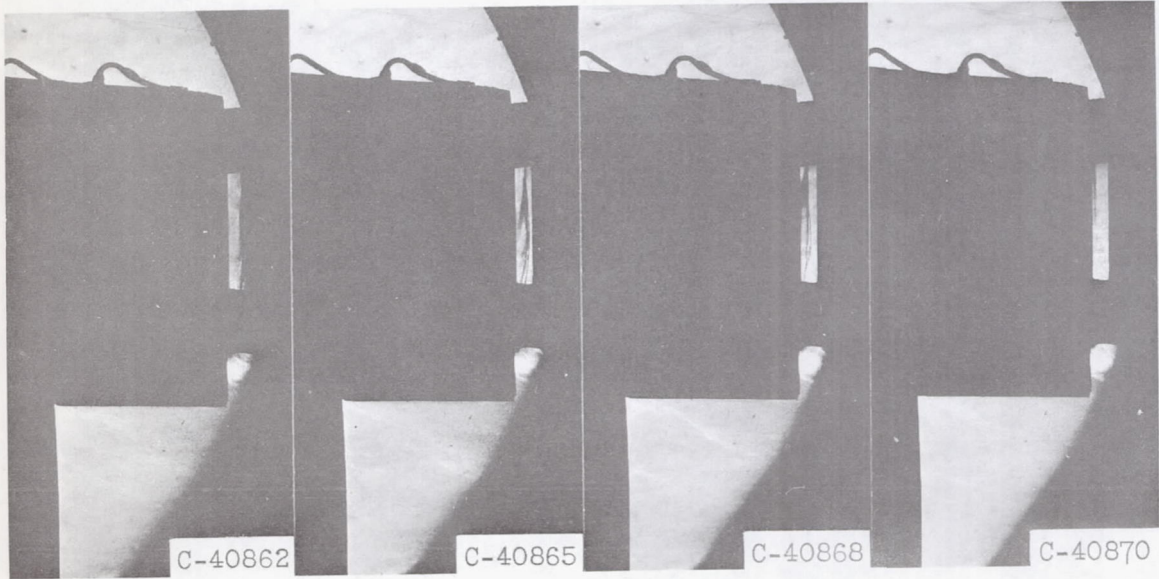
4857



→
Airflow

(a)

Inlet
throat



(b)

(c)

(d)

(e)

Figure 6. - Schlieren photographs showing terminal shock in bleed gap of fixed-capture-area-inlet. Mach number, 2.94.

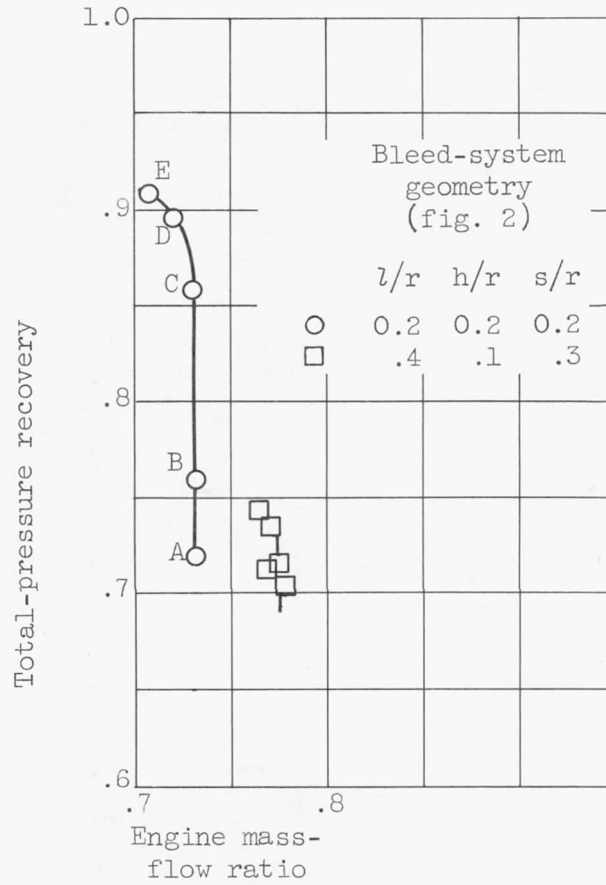


Figure 7. - Pressure recovery for variable-capture-area inlet with shock-trap bleed. Mach number, 2.94. (Letters refer to profiles of fig. 8.)

4857

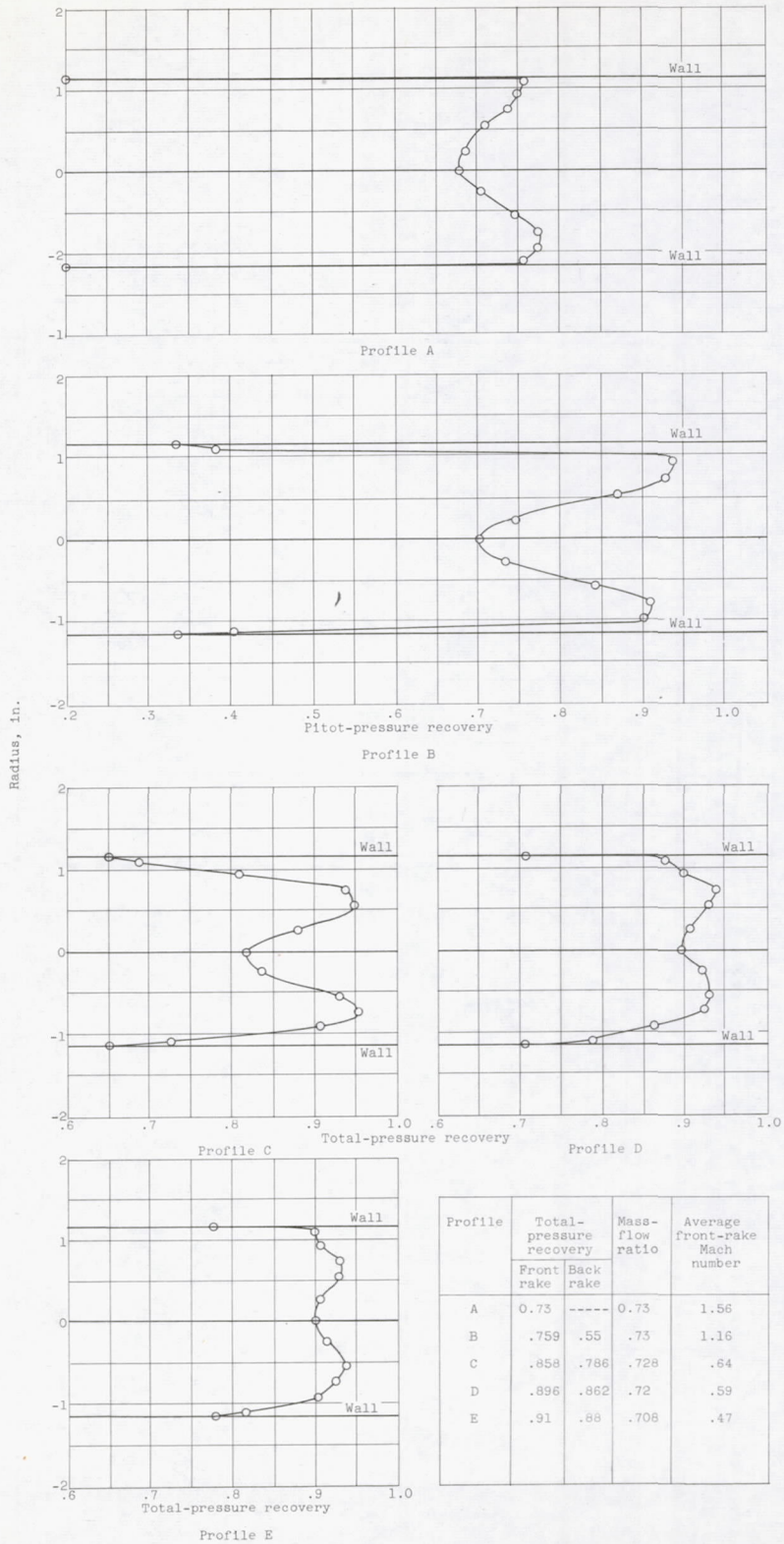


Figure 8. - Front-rake profiles for variable-capture-area inlet. Mach number, 2.94; $l/r = h/r = s/r = 0.2$ (see fig. 2).

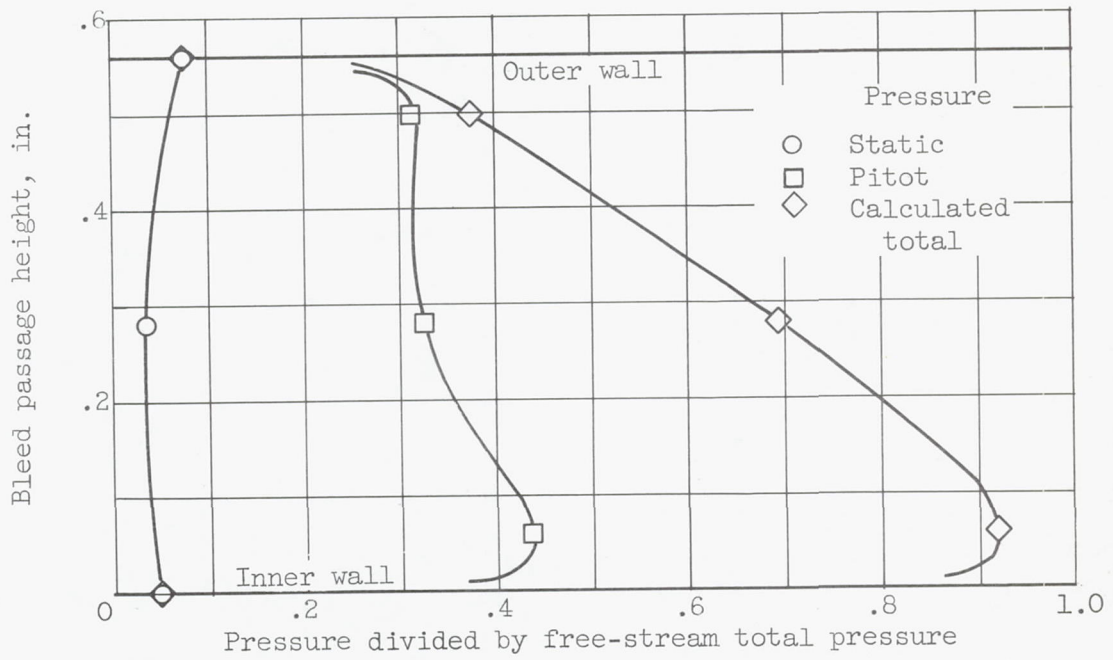


Figure 9. - Typical bleed-duct profiles for variable-capture-area inlet. Mach number, 2.94; $l/r = h/r = s/r = 0.2$ (see fig. 2).

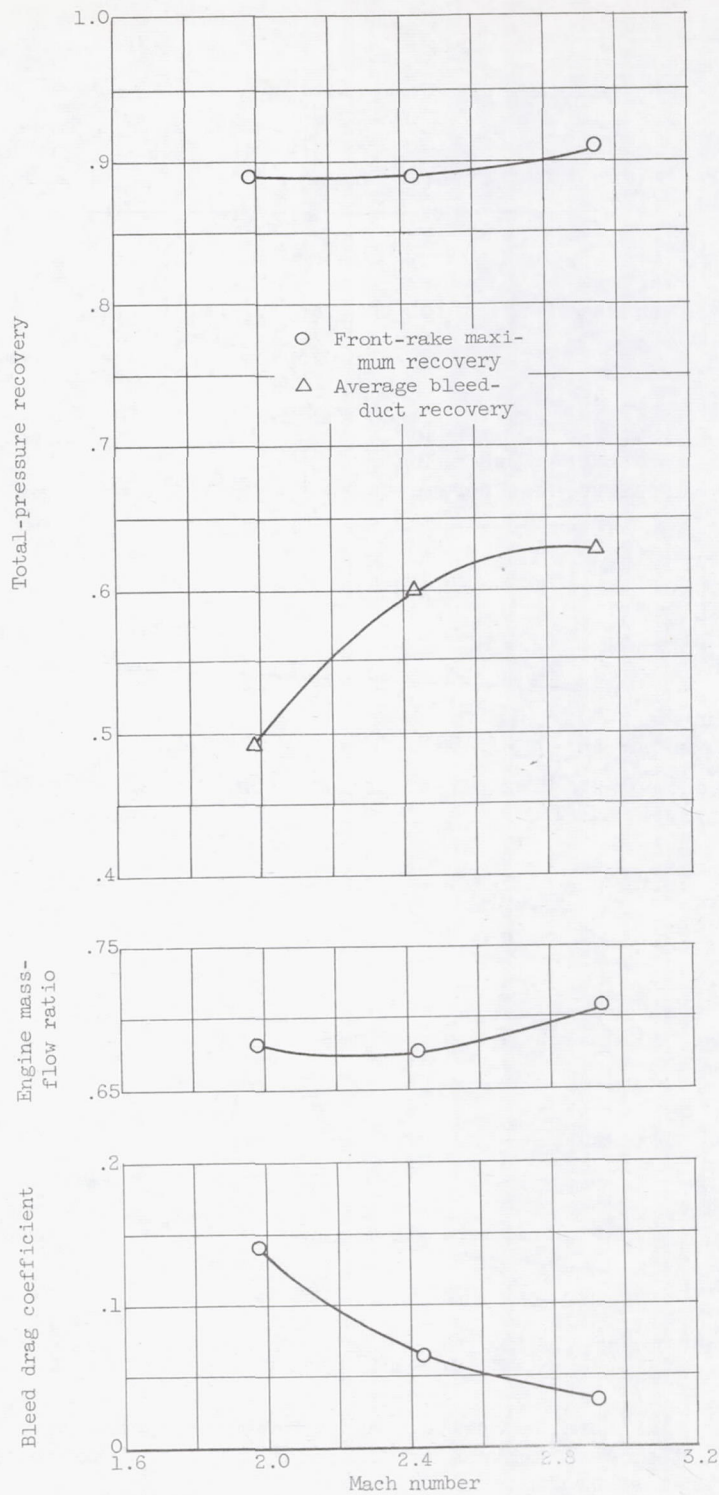
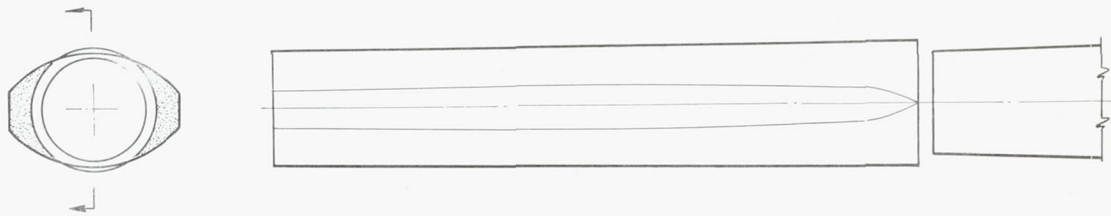
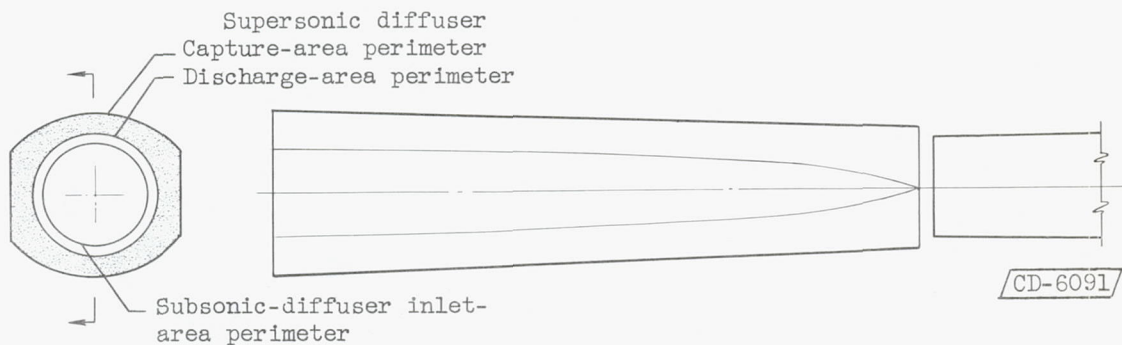


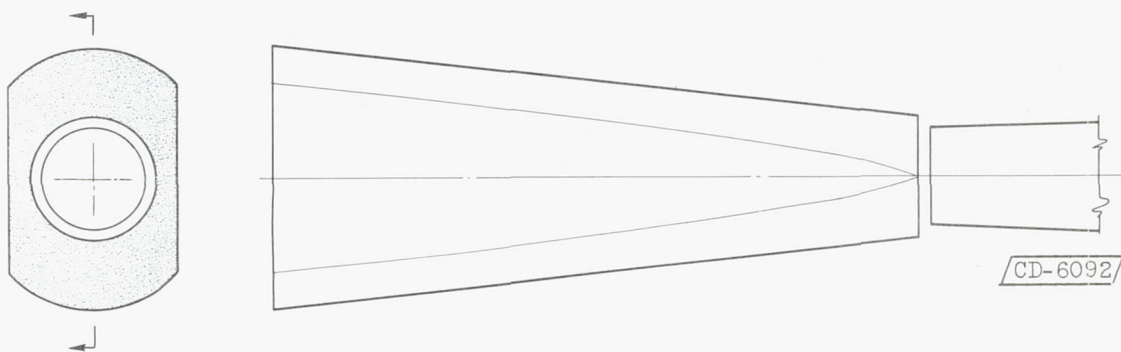
Figure 10. - Summary of performance of variable-capture-area inlet at maximum pressure recovery for several test Mach numbers.



(a) Mach number, 1.98; inlet contraction ratios: experimental, 1.35; isentropic, 1.66.



(b) Mach number, 2.43; inlet contraction ratios: experimental, 2.08; isentropic, 2.47.



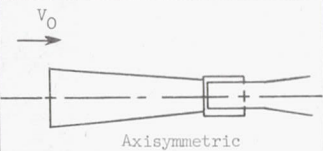
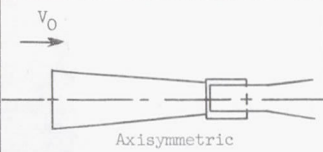
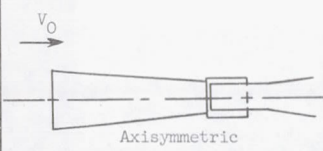
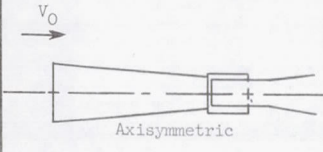
(c) Mach number, 2.94; inlet contraction ratios: experimental, 3.26; isentropic, 4.00.

Figure 11. - Schematic drawings of variable-capture-area-inlet model at several test Mach numbers. (Contraction ratio = Capture area/Supersonic-diffuser-discharge area.)

NOTES: (1) Reynolds number is based on the diameter of a circle with the same area as that of the capture area of the inlet.

(2) The symbol * denotes the occurrence of buzz.

INLET BIBLIOGRAPHY SHEET

Report and facility	Description			Test parameters				Test data			Performance		Remarks	
	Configuration	Number of oblique shocks	Type of boundary-layer control	Free-stream Mach number	Reynolds number $\times 10^{-6}$	Angle of attack, deg	Angle of yaw, deg	Drag	Inlet-flow profile	Discharge-flow profile	Flow picture	Maximum total-pressure recovery		Mass-flow ratio
CONFID. RM E58D24 Lewis 1- by 1-ft block tunnel		Multiple	"Shock-trap" bleed	2.94 2.43 1.98	1.3 1.6 1.3	0	0			✓	✓	0.91 .89 .89	0.71 .67 .68	A "shock-trap" bleed is a scoop bleed at the inlet throat with an area expansion starting upstream of the leading edge of the scoop. All spillage is through the bleed system.
CONFID. RM E58D24 Lewis 1- by 1-ft block tunnel		Multiple	"Shock-trap" bleed	2.94 2.43 1.98	1.3 1.6 1.3	0	0			✓	✓	0.91 .89 .89	0.71 .67 .68	A "shock-trap" bleed is a scoop bleed at the inlet throat with an area expansion starting upstream of the leading edge of the scoop. All spillage is through the bleed system.
CONFID. RM E58D24 Lewis 1- by 1-ft block tunnel		Multiple	"Shock-trap" bleed	2.94 2.43 1.98	1.3 1.6 1.3	0	0			✓	✓	0.91 .89 .89	0.71 .67 .68	A "shock-trap bleed is a scoop bleed at the inlet throat with an area expansion starting upstream of the leading edge of the scoop. All spillage is through the bleed system.
CONFID. RM E58D24 Lewis 1- by 1-ft block tunnel		Multiple	"Shock-trap" bleed	2.94 2.43 1.98	1.3 1.6 1.3	0	0			✓	✓	0.91 .89 .89	0.71 .67 .68	A "shock-trap" bleed is a scoop bleed at the inlet throat with an area expansion starting upstream of the leading edge of the scoop. All spillage is through the bleed system.

Bibliography

These strips are provided for the convenience of the reader and can be removed from this report to compile a bibliography of NACA inlet reports. This page is being added only to inlet reports and is on a trial basis.